"Coarse" stability and bifurcation analysis using time-steppers: A reaction-diffusion example

Constantinos Theodoropoulos*, Yue-Hong Qian†, and Ioannis G. Kevrekidis*‡

*Department of Chemical Engineering, Princeton University, Princeton, NJ 08544; and †Department of Applied Physics, Columbia University, New York, NY 10027

Communicated by Andrew J. Majda, New York University, New York, NY, May 15, 2000 (received for review April 10, 2000)

Evolutionary, pattern forming partial differential equations (PDEs) are often derived as limiting descriptions of microscopic, kinetic theory-based models of molecular processes (e.g., reaction and diffusion). The PDE dynamic behavior can be probed through direct simulation (time integration) or, more systematically, through stability/bifurcation calculations; time-stepper-based approaches, like the Recursive Projection Method [Shroff, G. M. & Keller, H. B. (1993) *SIAM J. Numer. Anal.* 30, 1099–1120] provide an attractive framework for the latter. We demonstrate an adaptation of this approach that allows for a direct, effective ("coarse") bifurcation analysis of microscopic, kinetic-based models; this is illustrated through a comparative study of the FitzHugh–Nagumo PDE and of a corresponding Lattice–Boltzmann model.

Introduction

Complex, spatially varying physicochemical processes are often accurately modeled by systems of partial differential equations (PDEs). Dissipative, pattern forming PDEs can arise as limiting descriptions (e.g. mean-field approximations) of the evolution of microscopic, kinetic calculations [Monte Carlo (MC), molecular dynamics (MD), or Boltzmann equation-based schemes]. The long-term dynamics of (discretizations of) these PDEs can be studied computationally through direct simulation (integration in time) of the corresponding large sets of coupled ordinary differential or differential algebraic equations. The same is true for microscopic models: long-term dynamics can be studied through extended direct simulation in time. A systematic analysis of the dynamics is, however, more efficiently performed in the PDE case through *numerical bifurcation calculations*, relying on the solution of large systems of algebraic equations. Such calculations are, in principle, not accessible to direct microscopic simulation codes. The purpose of this communication is to illustrate how the so-called "time-stepper-based" bifurcation algorithms for PDE discretizations can be adapted to perform the "coarse" bifurcation analysis of models for which only microscopic evolution rules are available.

PDE steady states and their dependence on parameters can be obtained through Newton's method and its implementation in continuation/bifurcation algorithms. This implementation is easy and efficient if the right-hand sides of the PDEs can be explicitly obtained. If a transient integration scheme (a "time-stepper") is available, it can be used to locate *stable* steady states after (possibly long) integration. Shroff and Keller (1) introduced a scheme, named the Recursive Projection Method (RPM), which is built around an existing time-stepper. Steady states of the PDE are found as fixed points of the time-stepper. The scheme, by repeatedly calling the time-stepper for several (nearby) initial conditions and for short periods of time, effectively converts an available, possibly complicated (e.g., split step) time-stepper into a bifurcation code with minimal programming effort. Exploiting the dissipative nature of the PDE and the concomitant separation of time scales, RPM treats the time-stepper as a black-box and adaptively identifies a low dimensional subspace **P**, along which time-evolution is slowest (even slightly unstable). It performs Newton iterations with a (small) approximate Jacobian **in** this subspace and Picard iterations on its orthogonal complement **Q**. These small Jacobians are, in principle, easy to invert. The procedure is well-suited for the bifurcation analysis of large systems close to low-codimension bifurcations, because it sidesteps the problem of constructing and inverting large Jacobians (see also refs. 2 and 3).

PDE ("coarse") steady states correspond to *stationary* profiles, in space, of moments (e.g., concentrations) of populations in microscopic simulations. In other words, "coarse" steady states can be thought of as projections of the stationary states of microscopic simulations. The exact *steady* (not stationary, but actually steady) states of, say, an MD simulation (e.g., all molecules having zero velocity and zero acceleration) are not necessarily the same (in fact we do not expect them to be) as the averaged, coarse steady states of interest here, for which fluctuations at the molecular level persist.

Traditionally, the parameter-dependent behavior of a system is analyzed by first obtaining a "coarse" model (e.g., a mean-field PDE) and then performing bifurcation analysis of the PDE. Here we propose to adapt RPM-type methods in order to perform "coarse" bifurcation studies using microscopic evolution rules directly, i.e., to perform "coarse bifurcation calculations" *without first explicitly constructing a "coarse" model*. The basic building block of the approach remains a call to a time-stepper. If a "coarse" model exists, this call involves (*i*) prescription of a "coarse" initial condition (concentration profile) and (*ii*) integration of the "coarse" model, the discretized PDE. The macroscopic time interval used (the time-stepper reporting horizon) is dictated by the dissipative nature of the PDE and corresponds to a natural separation between the "slow" and "fast" mode time scales (the gap between the corresponding linearization eigenvalues, see ref. 4). If the coarse model is not available, the evolution of a "coarse" initial condition (IC) can be obtained through (*i*) translating the coarse IC in one—or more—microscopic realizations consistent with it, (*ii*) evolving the realization(s) using microscopic rules for the same macroscopic time interval, and (*iii*) appropriately averaging the results *over fine space and/or fine time and/or number of realizations* to obtain the *coarse time-T map*. Thus, coarse concentration profiles can be evolved through either coarse model (discretized PDE) time-steppers or microscopic time-steppers. This conceptual procedure is illustrated in Fig. 1. The structure of the RPM-based "coarse bifurcation" code remains unchanged, and a coarse bifurcation analysis is performed even in the absence of an explicitly derived and discretized mean-field PDE (or other evolutionary rule). A vital point, of course, is the translation of a coarse IC to one or more consistent microscopic ICs. While a multitude of consistent microscopic ICs exist, our illustration was chosen to be relatively insensitive to this major issue.

Abbreviations: PDE, partial differential equation; RPM, Recursive Projection Method; MC, Monte Carlo; MD, molecular dynamics; IC, initial condition; FD, finite difference; LB, Lattice–Boltzmann; FHN, FitzHugh–Nagumo.

‡To whom reprint requests should be addressed.

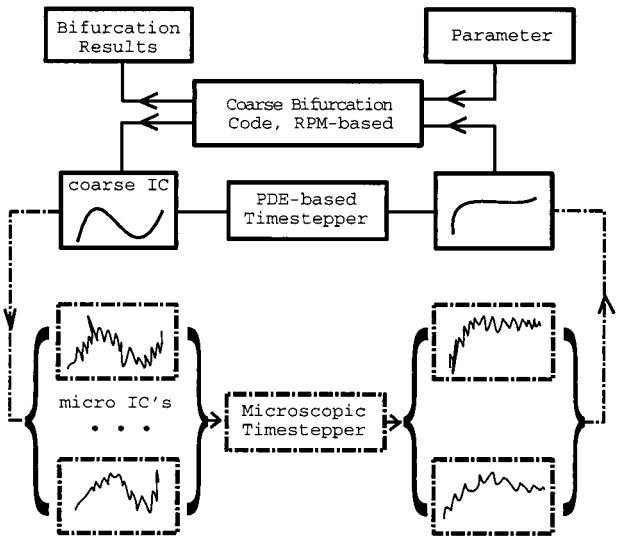

Fig. 1. Schematic of time-stepper-based bifurcation analysis for macroscopic and microscopic systems.

The Model

The example we chose to demonstrate the *coarse bifurcation analysis* concept is one where the mean-field PDE *is* available, in order to assess the performance of RPM applied to a "microscopic" time-stepper. We use a two-variable reaction-diffusion system, namely the FitzHugh–Nagumo model (FHN), in one spatial dimension (5–7):

$$u_t = u_{xx} + u - u^3 - v \quad [1]$$

$$v_t = \delta v_{xx} + \epsilon(u - a_1 v - a_0) \quad [2]$$

In pattern formation terminology, u is the *activator* and v the *inhibitor* concentration.

The kinetic parameter values chosen are $a_0 = -0.03$ and $a_1 = 2.0$; $\delta = 4.0$ is a diffusion coefficient. The time-scale ratio, ϵ, is our bifurcation parameter; both a Hopf and a saddle-node bifurcation arise in this particular one-parameter diagram. Stability/bifurcation calculations were performed through (*i*) a standard finite difference (FD) discretization, direct linear algebra steady solvers, and standard Newton/continuation techniques, for reference; (*ii*) RPM implemented around an (implicit Euler) time-stepper of the same FD spatial discretization, for confirmation; and (*iii*) RPM implementated around a "microscopic" Lattice–Boltzmann (LB) simulator of the same system.

LB models (8, 9) were introduced as an alternative to the macroscopic description of hydrodynamic systems; they lack the statistical noise inherent in lattice-gas models, but they are still conceptually simple and easily amenable to computational implementation and solution. The LB models are based on a finite difference-type disretization of the continuum Boltzmann–BGK equation (10), which describes the evolution in space and time of a single particle distribution function. Particle transport in LB consists of streaming (particles moving towards adjacent sites in a lattice of fixed size), and of (non-reactive) collisions (particles colliding at a site). In the LB–BGK model we have implemented for the reaction-diffusion system the evolution equations for u are (11):

$$N_i^u(x + c_i, t + 1) - N_i^u(x, t) = -\omega^u[N_i^u(x, t) - N_i^{u,e}(x, t)] + R_i^u(N_j^u, N_k^v) \quad [3]$$

(and correspondingly for v). Here, $N_i^u(x, t)$ is the population density of activator (u) particles at position x on the lattice at time t, with velocity c_i. In this one-dimensional system, particles can move only toward the two available adjacent sites (N_2, N_3) or (allowing for rest particles) stay in place (N_1). For unitary LB temporal and spatial increments, therefore, $c_i = \{0, 1, -1\}$ and $i = 1, 2, 3$ respectively. $N_i^{u,e}$ is the local equilibrium u population, homogeneous in all velocity directions, and ω^u is the BGK relaxation parameter; the first part of the right-hand side computes post-collision populations. R_i^u is the reaction term; we use the (strong) assumption (11) of local diffusive equilibrium for the reaction term. The left-hand side computes the particle *streaming*. In this case, there are 2 concentrations (u,v) at each lattice site and 3 discrete possible velocities per concentration (6 population densities overall). While concentrations can be uniquely computed as the 0th moments of the populations, e.g.,

$$u(x, t) = \sum_{i=1}^{3} N_i^u(x, t), \quad [4]$$

the opposite is not true. If a "coarse" initial condition (concentrations, zeroth moments) is specified, any 3 random numbers (weights) w_i summing up to 1 would be a possible choice, i.e.,

$$N_i^u(x, t) = w_i u(x, t). \quad [5]$$

It so happens that in our LB–RPM the choice of initial weights is not critical; initial disturbances caused by such random choices decay much faster than the (macroscopic) time interval used in the time-stepper (as we will discuss below).

Results and Discussion

We first constructed the bifurcation diagram of a detailed FD discretization of the FHN model, to benchmark our RPM time-stepper calculations. For a domain of length $L = 20.0$ with 200 discretization nodes, a Hopf bifurcation was found at $\epsilon \approx 0.015$ and a saddle-node at $\epsilon \approx 0.944$; the one-parameter diagram is shown in Fig. 2, where $\langle u \rangle$, the spatial average of u, is plotted against ϵ.

We then implemented an RPM-continuation code around a time-stepper employing an implicit Euler scheme for this discretization. The time-stepper reporting horizon, T, should correspond to a time scale long enough for the fast modes (but not the slow stable ones) to decay; for our problem T ranged from 15 to 25. Let us clarify that this is not an economic alternative to direct bifurcation calculations for this problem; a single implicit integration step clearly costs as much as a direct steady

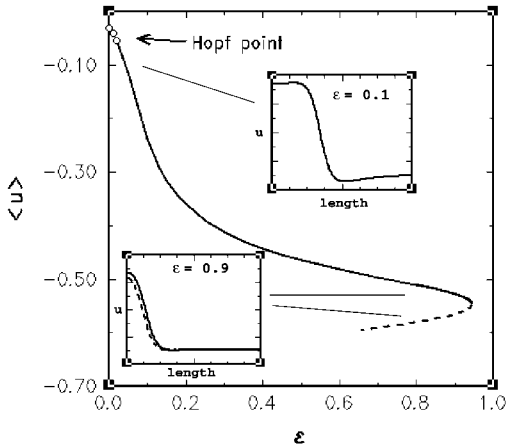

Fig. 2. Bifurcation diagram (spatial average $\langle u \rangle$, vs. ϵ) of the one-dimensional FHN equations. Solid (dashed) line, stable (unstable beyond turning point) steady states; open circles, unstable steady states beyond the Hopf bifurcation. (*Insets*) Steady state profiles $u(x)$ at representative ϵ values.

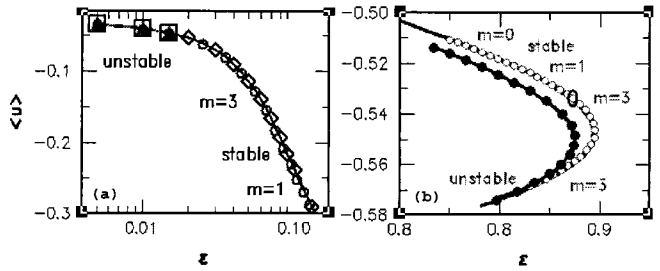

Fig. 3. Blow-ups of the bifurcation diagram (*a*) near the Hopf point. Steady FD code (FD-SS), stable branch (open diamonds), unstable (open squares); FD time-stepper with RPM (FD-RPM), stable branch (solid line), unstable (filled triangles); LB time-stepper with RPM (LB-RPM), stable branch (open circles), unstable (filled circles). (*b*) Near the saddle-node bifurcation. FD-SS (solid line), FD-RPM (open circles), LB-RPM (filled circles).

state calculation; it is only done for RPM benchmarking. In the RPM implementation around this time-stepper the dimension of the subspace **P** was increased (by 1 or 2, depending on whether one or two additional eigenvalues became "large" enough to impede convergence). RPM enabled the time-stepper to converge to unstable portions of the steady state branches, both beyond the Hopf (Fig. 3*a*) and the turning point bifurcations (Fig. 3*b*), and reproduce the bifurcation diagram. The dimension, m, of **P** ranged from m = 0 (far from the instabilities) up to m = 3 as the instabilities were approached; the size of the reduced Jacobians was therefore minimal (up to 3×3).

A Lattice–Boltzmann time-stepper was then implemented to study the dynamics of the LB–FHN model. The lattice considered here had 400 sites. The model performance was first tested against FD-based integrations. The spatiotemporal behavior of $u(x, t)$ on a limit cycle computed through the FD and the LB time-steppers (at $\epsilon = 0.006$) is depicted in Fig. 4 *a* and *b*, respectively; the agreement is very good. Performing long, transient LB simulations for different values of ϵ, steady states of the system can be computed, but only on the stable branch (see Fig. 4*c*). The LB model, predicts (especially at higher values of ϵ) slightly different stationary spatial profiles for u (and v) from the steady state profiles of the FD code; the relative difference here is of the order of $\sim 1\%$, comparable with the FD discretization error.

As mentioned above, a systematic way of converting nearby coarse (macroscopic) initial conditions to consistent ICs of the microscopic integrator is a vital issue for coarse stability calculations via RPM. A number of (reasonable) different LB initializations was tested to ensure the robustness of the RPM process. We had to translate 400 numbers (two concentrations at 200 points each) to 2,400 numbers (three densities each for two quantities at 400 lattice points, respectively). All of our initialization tests were performed for $\epsilon = 0.8$, starting from a "coarse" steady state profile on the stable branch, obtained by 200-node FD simulations at a nearby parameter value ($\epsilon = 0.5$). We used three equal weights in Eq. 4 as well as random weights summing up to 1. We performed both "fine" and "coarse" initializations. For "fine" initializations, starting from the (interpolated) steady state coarse concentration profile, three equal weights ($w_i = 1/3$) were first used as in Eq. 5 to initialize each population at each lattice site. Triads of random weights (w_i) with sum 1, different for each site, were also employed. For coarse initializations, starting from the same coarse steady state profile, locally averaged values of u and v ($\overline{u}$ and $\overline{v}$) every 10 consecutive FD nodes were calculated. These averages were used to initialize (in a "step" fashion) the corresponding lattice site populations through both equal and random weights. Even in the more severe "coarse" case with random weights, the discrepancy between (the projections on the zeroth moments of) different trajectories, caused by the different initializations, were practically eliminated after times much shorter than the RPM-time-stepper reporting horizon (after $t \approx 0.1$ as compared to $T = 15 - 25$).

The LB time-stepper was then coupled to RPM, taking enough microscopic collision/streaming steps to match the macroscopic reporting horizon. The LB–RPM "microscopic" system was able to accurately reproduce the "coarse" PDE bifurcation diagram in the neighborhood of the Hopf bifurcation (Fig. 3*a*). Both stable and unstable branches converged on, were essentially the same as the steady states computed through the "coarse" code (the FD PDE discretization). This also holds in the neighborhood of the saddle-node bifurcation; in this case the discrepancy between the stationary states of the LB–RPM and the steady states of the PDE was slightly more pronounced.

A natural byproduct of RPM-type methods applied to a discretized PDE time-stepper is the leading eigenspectrum of the PDE Jacobian, reconstructed from the eigenvalues and eigenvectors of the small Jacobian in the slow subspace. The eigenvalues μ_i of this small "coarse Jacobian" at a fixed point of the time-stepper are related to the eigenvalues λ_i of the "full" coarse Jacobian of the system: $\mu_i = \exp(\lambda_i T)$. An attractive feature of the LB–RPM technique is that it correspondingly approximates the leading "coarse" eigenspectrum of the system in question, from the approximated small "coarse" Jacobian. In these simulations the dimension of this small Jacobian ranged from 0 to 3. RPM also accurately predicted the value of ϵ where eigenvalues cross the imaginary axis (here ~ 0.015). Finally, the leading eigenvectors of the system linearization were also successfully reconstructed. They are depicted in Fig. 5 *a* and *b* for $\epsilon = 0.01$. In all cases the eigenvectors compare well with the

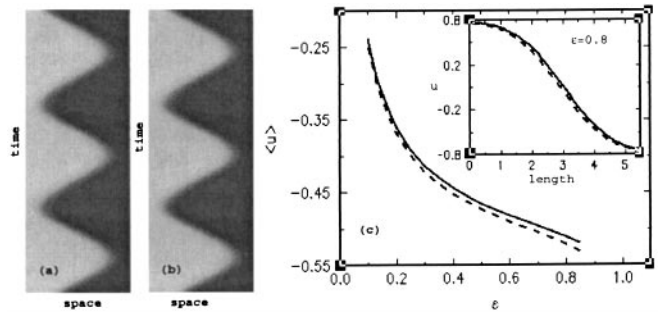

Fig. 4. Spatiotemporal behavior of u on a limit cycle ($\epsilon = 0.006$) computed by LB (*a*) and FD (*b*) time-steppers. Dark (light) gray corresponds to higher (lower) concentrations of u. (*c*) Comparison of FD-SS (solid line) and LB (dashed line) steady states. (*Inset*) The front portion of the steady state $u(x)$ profile, computed through FD-SS (solid line) and LB (dashed line).

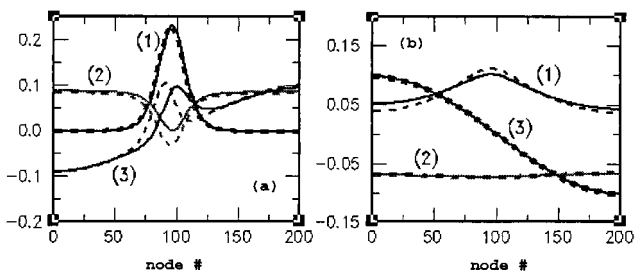

Fig. 5. (*a*) u- and (*b*) v-components of leading eigenvectors for $\epsilon = 0.01$: FD-SS (solid lines) and corresponding coarse LB-RPM (dashed lines). Pairs 1 and 2, real and imaginary part of the leading eigenvector. Pair 3, eigenvector of the next (real) eigenvalue.

ones from the FD code despite the fact that they were reconstructed from a small (three-dimensional) LB simulation-based subspace.

Conclusions

What was illustrated here for LB-based time-steppers can, in principle, also be accomplished for other microscopic (MC, MD) or hybrid simulators [e.g., CONNFFESSIT, Brownian configuration fields (12–14), and DSMC (15)]: the action of the (coarse) Jacobian on the presumably low-dimensional subspace of slow (or slightly unstable) coarse system modes can be approximated through a (microscopic) time-stepper and used in (macroscopic, "coarse") bifurcation calculations. The use of repeated, relatively short-term calls to the microscopic/hybrid time-stepper sidesteps the necessity of deriving (and closing) a macroscopic (coarse) equation for the system moments. What the approach extracts from the microscopic time-stepper is precisely the minimal information required to perform the computational bifurcation analysis of a coarse PDE (or other types of coarse deterministic evolution rules). Vital issues for the success of the scheme are (*i*) the translation of coarse initial conditions to "good" consistent microscopic realizations, and (*ii*) averaging (if necessary) the evolution result of these microscopic ICs over fine space and/or fine time and/or realizations to obtain the corresponding coarse short term integration result (an accurate *coarse time-T map*). We believe that the approach holds promise for the systematic stability and parametric analysis of the coarse dynamic behavior of a large class of systems described through microscopic evolution rules. In a similar spirit (averaging "detailed" time-stepper results over realizations of heterogeneous media rather than microscopic time-stepper results over microscopic initial conditions) it may also play a role in the stability/parametric analysis of the coarse dynamic behavior of phenomena in complex media for which effective equations are difficult to obtain [e.g., reaction and diffusion on composite catalysts (16)].

This work was partially supported by the Air Force Office for Scientific Research, Sandia National Labs and UTRC.

1. Shroff, G.M. & Keller, H.B. (1993) *SIAM J. Numer. Anal.* **30,** 1099–1120.
2. Jarausch, J. & Mackens, W. (1984) in *Numerical Methods for Bifurcation Problems*, eds. Küpper, T., Mittelman, H. D. & Weber, H. (Birkhäuser, Basel).
3. Tuckerman, L. S. & Barkley, D. (1999) in *IMA Volumes in Mathematics and Its Applications*, eds. Doedel, E. & Tuckerman, L. S. (Springer, New York) Vol. 119, pp. 453–466.
4. Davidson, B. D. (1997) *SIAM J. Numer. Anal.* **34,** 2008–2027.
5. FitzHugh, R. (1961) *Biophys. J.* **1,** 445–466.
6. Nagumo, J. S., Arimoto, S. & Yoshizawa, S. (1962) *Proc. IREE* **50,** 2061–2070.
7. Murray, J. D. (1989) *Mathematical Biology* (Springer, New York).
8. Benzi, R., Succi, S. & Vergassola, M. (1992) *Phys. Rep.* **22,** 145–197.
9. Rothman, D. H. & Zaleski, S. (1997) *Lattice-Gas Cellular Automata. Simple Models of Complex Hydrodynamics* (Cambridge Univ. Press, Cambridge, U.K.).
10. Bhatnagar, P., Gross, E. P. & Krook, M. K. (1954) *Phys. Rev.* **94,** 511–525.
11. Qian, Y. H. & Orszag, S. A. (1995) *J. Stat. Phys.* **81,** 237–253.
12. Laso, M. & Öttinger, H. C. (1993) *J. Non-Newtonian Fluid Mech.* **47,** 1–20.
13. Jendrejack, R. M., de Pablo, J. J. & Graham, M. D. (2000) in *Proc. XIIIth Int. Cong. Rheology*, eds. Binding, D. M., Hudson, N. E., Mewis, J., Piao, J.-M., Petrie, C. J. S., Townsend, P., Wagner, M. H. & Walters, K. (British Society of Rheology, Glasgow, U.K.), pp. 2-214–2-216.
14. Öttinger, H. C., vandenBrule, B. H. A. A. & Hulsen, M. A. (1997) *J. Non-Newtonian Fluid Mech.* **70,** 255–261.
15. Bird, G. (1994) *Molecular Gas Dynamics and the Direct Simulation of Gas Flows* (Clarendon, Oxford).
16. Shvartsman, S. Y., Shütz, E., Imbihl, R. & Kevrekidis, I. G. (1999) *Phys. Rev. Lett.* **83,** 2857–2860.